Design Considerations for Artificial Water Channel based Membranes

Woochul Song[1], Chao Lang[1], Yue-xiao Shen[2], and Manish Kumar*[1, 3, 4]

[1] Department of Chemical Engineering,[3]Department of Biomedical Engineering,[4] Department of Civil and Environmental Engineering, The Pennsylvania State University, University Park, PA, 16802 USA

[2] Department of Chemistry, University of California, Berkeley, CA,94720 USA

Email addresses

woochul.song@psu.eduWoochul Song

cul389@psu.edu Chao Lang

syxbach@berkeley.edu Yue-xiao Shen

*To whom correspondence should be addressed.

Tel.: (814)-865-7519

Email: manish.kumar@psu.edu

ABSTRACT

Aquaporins(AQPs) are naturally occurring water channel proteins, which can facilitate water molecule translocation across cellular membranes with exceptional selectivity and high permeability that are unmatched in synthetic membrane systems. This unique property of AQPs has led to their use as functional elements in membranes in recent years. However, the intricate nature of AQPs, and concerns regarding their stability and processability has encouraged researchers to develop synthetic channels that mimic the structure and properties of AQPs and other biological water conducting channels. These channels have been termed artificial water channels. This article reviews current progress, provides a historical perspective and an outlook towards developing scalable membranes based on artificial water channels.

KEYWORDS

Artificial water channels, Aquaporins, Biomimetic membranes, Membrane fabrication, Membrane based separations

1. INTRODUCTION

Synthetic membranes have assumed a central role in the area of separation of molecules and particles in recent years. Large-scale applications currently include water purification and recycling, biopharmaceutical manufacturing, food and dairy applications (1-4). Proposed uses can be extended to specific gas and small molecule separations that in many cases could reduce the energy burden of phase changes based on distillation (2, 5, 6). As an example, for desalination, although both thermal technologies (such as multi-stage flash distillation) and membrane-based technologies have been implemented, membrane-based technologies are becoming the dominant technology in recent years. This is due to the structural simplicity (compact and modular), low energy consumption, and low chemicals usage (5, 7-9) of membrane technologies. However, despite these advantages, the most challenging separations for membranes have been at the Angstrom scale where separations for ions, gases, and small molecules occur. In this size range, polymeric membranes that perform well in other size ranges suffer more from the challenge of the permeability-selectivity trade-off, i.e. reduced selectivity at high permeability and vice versa. Polymeric membranes used for such separations are considered non-porous with no straight through pores or channels, instead chemical species travel through the polymers by first dissolving and then diffusing through the polymers. The permeability-selectivity trade-off observed originates from this solution-diffusion transport (10) occurring through free volume elements of variable sizes and reflect the non-ideality of current membranes that lack well defined pore sizes (5).

In contrast to synthetic membranes, biological membranes that are responsible for transport of water and exclusion of Angstrom-scale solutes in cells have high permeability while maintaining high selectivity (11). This combination of permeability and selectivity is primarily due to the presence of specialized membrane proteins that mediate transport across

cell membranes. These membrane proteins have an ideal monodisperse pore size and additional mechanisms such as charge based exclusion as well as specific binding. An excellent example of a highly selective but permeable membrane protein is the class of water channel proteins known as aquaporins (AQPs) (12, 13). Classical AQPs are only permeable to water while excluding all solutes (including ions and protons) while maintaining a high permeability of 10^9 H_2O molecules/s/channel. It has an hour glass pore profile with a narrow constriction of ~ 3Å that prevents solutes from entering the pore. It also has a highly charged arginine residue towards the entrance of the pore and a set of conserved residues in the central part of the pore that "flips" the orientation of any passing water molecule through a series of hydrogen bonding steps (13). This reorientation leads to an interruption of the proton wire and decouples water transport from proton transport, thus completely inhibiting protons from crossing the membrane through the channel (13, 14). Due to its unique transport properties, AQPs have been incorporated into membrane matrices for applications in desalination and water purification (11). However, high costs, difficulties in fabrication, and low stability associated with membrane protein-based materials have hampered the large-scale applications of AQP-based membranes (11, 15).

An alternative to synthesizing high performance membranes based on AQPs and other membrane proteins is the use of synthetic mimics of these biological channels. In particular, synthetic channels created using organic chemistry that mimic the structures and functions of AQPs and other water conducting biological channels have emerged and come to be known as artificial water channels (16, 17). These channels provide several advantages over biological channels, particularly when fabrication of scalable membranes for applications is considered. They can be synthesized using simple chemical techniques and dissolved in solvents to allow for large-scale conventional processing of membranes as currently practiced. They can also be functionalized using a host of techniques allowing for further enhancements

in selectivity while maintaining permeability (18-21). There has been a large interest in recent years in developing membrane materials based on these artificial water channels (16, 17). This review specifically aims to describe the progress and prospects for developing separation membranes around artificial water channels. The early sections introduce the synthesis, structure, and properties of currently known artificial water channels; and later sections describe the characteristics of ideal water channels for development into membranes. The final sections shed light on the design considerations for membrane fabrication around artificial water channels, which is followed by a few possible designs that are evident based on currently used designs for AQP-based membranes and our own work.

2. ARTIFICIAL WATER CHANNELS

Artificial water channel based membrane research aims to emulate biological membrane components with practical synthetic models while maintaining their outstanding molecular separation properties. Artificial water channels currently being researched can be classified into two main types: self-assembling channels and unimolecular channels(16, 22). In this section, we review synthetic water channels, considering their design strategies and resultant transport properties.

2.1. Self-assembling channels

Dendritic dipeptide pores

Dendritic dipeptide aquapores are among the first known successful synthetic water channels. They were proposed by Percec and coworkers in early 2000s (Figure 1, **1A**) (23, 24)and included a library of amphiphilic dendritic dipeptides, which can self-assemble into helical columnar structures with internal open pores of 12.8 ± 1.2Å (Figure 2b). The structural integrity of these helical pores was ensured by successful hydrogen bond (H bond) formation

between dipeptide dendrons. Therefore, these dendritic monomers could assemble into integral pore conformations only in non-polarized H bond free media, including cyclohexane or the aliphatic (hydrophobic) compartment of lipid bilayers, rather than in polarized solvents including chloroform ($CHCl_3$), dichloromethane (CH_2Cl_2) or tetrahydrofuran (THF). Water transport abilities of these first artificial water channels were successfully demonstrated experimentally by reconstituting the channels into vesicular lipid bilayers (liposomes) and monitoring the translocation of protons acrosslipid bilayers via pH sensitive fluorescent dyes. These dendritic pores showed proton permeability comparable to the gramicidin A (gA) biological proton channel, a well-characterized membrane protein(25-27). Also, since proton transport is known to be accompanied by water transport, this result strongly indicated that the dipeptide pores can mediate water transport across lipid bilayers(28).

Even though the dipeptide pores showed remarkable progress as a‘primitive mimic of AQPs’, they suffered from low thermal stability due to dynamic equilibrium states of dendron monomers between trans and gauche conformers at around 22 °C (23). Later, to overcome this thermal instability, the benzyl ether moiety of dendrons was replaced by naphthyl groups which were located at the periphery of helical pores to induce π-π stacking interactions so that the entire structure could be stabilized (Figure 1, **1B**) (24). In the bulk state, these modified aquapores showed slightly enlarged pore diameters of 14.5± 1.5Å compared to the unmodified pores (Figure 2b), with enhanced thermal stability from 20 °C to 40 °C and, as a result, improved incorporation efficiency into lipid bilayers. Thermally stabilized dendritic aqua pores showed selective water and proton transport over Li^+, Na^+ and Cl^- monovalent ions which was attributed to hydrophobic effect near the channel entrance rather than steric hindrance.

Imidazole quartet channels

Influenza A M2 proton channels are model membrane proteins, which facilitate water and proton diffusion through water-filled pores. The transport characteristics of M2 proton channels have been related specifically to the imidazole quartet motif in the histidine quartet selectivity filter(29-33). Inspired by this structure, Barboiu and coworkers synthesized imidazole-quartet (I-quartet) channels (19, 34). They designed ureido imidazole compounds and demonstrated that these compounds can be crystalized into bulk states as well as self-assembled into transmembrane pore structures in lipid bilayers, forming dipolar water wire arrays inside the tubular imidazole architectures (Figure 2). These water-filled pores have an inner diameter of 2.6 Å and are stabilized by continuous and repetitive H-bonds between water molecules and imidazole moieties. These regular water arrays enable continuous water and proton conduction throughout the pores but reject other ions. From the structural perspective, a characteristic feature of I-quartet channels is that the entire conformation assembled within dynamic lipid bilayers could be affected by differences in the alkyl chains which are grafted onto the I-quartets, resulting in significant transport performance differences (Figure 2b). For example, as the length of alkyl chains increased, the water conduction rates increased substantially due to hydrophobic stabilization effects at the interface between imidazole and aliphatic compartment of the lipid bilayer. In addition, I-quartet channels showed different permeabilities depending on the chirality of the alkyl chains. It is hypothesized that naturally existing L-lipids are more compatible for specific chiral conformation in stabilizing the entire channel structure and a specific orientation of water wire arrays that leads to enhanced conduction. For the most optimal I-quartet channels (Figure 2h, **S-HC8**), single channel water permeability was calculated at ~ 1.5 $\times 10^6$ H_2O molecules/s/channel, which is only two orders lower than that of the classical mammalian AQP, AQP-1. Single channel proton conduction rate was ~ 5 H^+ molecules/s/channel which is ~50 % of the M2 proton channel transport rate. The I-quartet system is the first class of

synthetic water channels, which can reject all ions but mediate water and proton conduction. This property is explained by its restricted pore structure, which is compatible with water molecules (2.7Å), suggesting that ~ 3 Å is critical pore diameter for the future desalination applications of artificial channel based membranes.

Triazole channels

Gramicidin-A (gA) is another archetype of membrane proteinsthat demonstrates efficient water, proton, and ion conduction through biological membranes(25-27). As a primitive mimic of gA, synthetic triazole channels (T-channels), which are formed by assembly of the super structure of bola-amphiphile-triazole compounds (TCT), were proposed(Figure 3)(35).T-channels have many characteristic features comparable with gA in terms of pore diameter, conduction rates and ion selectivity. The crystal structure of T-channels showed, on average, 5Å diameter pores which are made of a TCT double helix and stabilized by intermolecular H bonds (Figure 3b).The pores form hourglass shapes via repeated tight (d = 2.5 Å) and large (4 Å) free void openings, encapsulating inversely oriented four dipolar water wires that are stabilized by H bonds between both of neighboring water molecules and inner walls of the TCT complex (Figure 3c).In terms of cation conduction rates, conventional ion channels have been known to follow the Eisenman sequence I ($Li^+ < Na^+ < K^+ < Rb^+ < Cs^+$) which is attributed to the dehydration energy penalty of fully hydrated cations in water and, therefore, has a linear relationship between hydration energy and conduction rates (Figure 3d)(36). However, interestingly, T-channels showed an abrupt conduction rate increase between Rb^+ and Cs^+, having single order exponential behavior in cation conduction rates ($Li^+ < Na^+ < K^+ < Rb^+ << Cs^+$) (Figure 3d).To elucidate this exceptional trend, Monte Carlo simulation was introduced and the simulation results revealed that the inner surface of the channels are highly hydrated with four continuous water wires and these steric water wire

conformations work as a sort of lubricant for small cations such as Cs^+, by hindering direct interactions between cations and inner surface of the channels, enhancing their conduction rates. In terms of anion conduction rates, T-channels showed two orders lower transport rates for Cl^- compared to Na^+, because the dipolar distribution of aligned water molecules is more favorable for dehydrating cations rather than anions.

Hexa(m-phenylene ethynylene) channels

Planar macrocycles have been regarded as promising building blocks to construct columnar nanopores that are less than 2 nm in diameter with a straight forward strategy of stacking them co-axially (37). Similar to this concept, several macrocycles, based on arylene ethynylene (38-40), aryl amide and hydrazide (41) backbones have been proposed as excellent candidates, but achieving satisfactory self-assembled structures in terms of uniformity, rigidity and practical performance has been challenging (42). Gong *et al.* have introduced a series of macrocycles which share a core structure of hexa(*m*-phenylene ethynylene) (*m*-PE) (Figure 4a) (42). They demonstrated that *m*-PE macrocycles can be efficiently stacked into columnar structures in solid state and solvent phases as well as in lipid bilayers (Figure 4b -d). Especially inside lipid bilayers, about 9 to 10 *m*-PE based macrocycles were stacked and stabilized by H bonds as well as π-π stacking interactions to form tubular nanopores. This number was in reasonable agreement with the thickness of lipid bilayers (~4 nm) since each π-π stacking distance was estimated to be ~3.6 Å. This self-assembled nanotube showed an inner pore diameter of 6.4 Å with outer diameter of ~3.7 nm. Also, *m*-PE incorporated vesicular membranes showed substantial water conductance rate along with the inner pores with approximately 22 % efficiency of AQP-1 incorporated liposomes, even though the single channel permeability is still not clear. In terms of ion selectivity, a significantly higher ratio between H^+ to Cl^- was observed (P_{H^+}/P_{Cl^-}= 3000)

than that of natural influenza M2 proton channel (P_{H^+}/P_{Cl^-}= 19.7) (43). Additionally, no significant Na^+ and Li^+ ion conduction was detected, implying that the energy cost for dehydration is also important in mediating ion conduction as seen in the case of the T-channels (35).The distinctive feature of *m*-PE channel is that they are amenable to structural decorations via chemical ligand modifications. For example, inside the pore, the aromatic protons could be replaced with methyl groups (Figure 4a, **2C**) and this resulted in reduced proton conduction rate due to steric hinderance. Also, the outer most alkyl chains could be extended from $-C_4H_9$ to $-C_8H_{17}$ (Figure 4a, **2B**) without any conformational disruption of columnar pores (Figure 4c and d).

Aquafoldamers

A class of macro folding molecules (foldamers) are known to have specialized properties with regard to selective molecular recognition (44-59). These distinctive properties inspired Zeng and coworkers to design pyridine based foldamers (Figure 5, pentamer **3**), which have high affinity to capture water molecules and to build up stacked tubular pores as mimics of AQPs, which they named ‘aquafoldamers’ or ‘aquapores’(60, 61). After years of investigation, they revealed that pentamer **3** has a helical 3D structure with 2.8-Å central columnar cavity which is very comparable with AQP’s narrowest region. To efficiently build up this foldamer in a one dimensional manner, they attempted several design strategies including changing pyridine repeat numbers (pentamer and hexamer) and introducing different ‘sticky ends’ (flexible carboxyl benzeneand rigid phenyl ring) at both ends of foldamers to elongate the helical structure, and concludedthat pentameric foldamer **4** wasthe most promising structure for application as a synthetic water channel (60). This pentamer **4** is composed of two sticky ends, one is an ester and another is rigid phenyl ring, which can intermolecularly interact with each other by H bonds and elongate the overall helical

structure for spanning the lipid bilayer (Figure 5a).Consequently, this foldamer could be assembled into chiral and helical transmembrane pores encapsulating two water molecules per repeating helical unit, as expected in crystal structure of un-assembled pentamer **3** and **4** (Figure 5b and 5c). The driving force to stabilize the entire pore structure is aromatic stacking of pyridine monomers. In addition, mutual interactions between sticky ends and synergistic hydrogen bonds of trapped water wires contributed to maintaining1D columnar stacks (Figure 5d). Inside the lipid bilayer, these aquapores showed substantial proton conduction across the bilayer membranes when higher proton concentration was imposed at the one side of membranes (specific values were not reported). Interestingly, the proton diffusion driven by concentration gradient drove water molecule translocation at the same time. This 'proton gradient-induced water transport' is a strong and empirical evidence of 1D water wire formation inside the aquapores crossing the lipid bilayers.

Triarylamine channels

Triarylamine-based synthetic water channels were initially derived from attempts to design synthetic ion channels that mimicked potassium channel (KcsA) proteins (62). Together with the fact that 1) triarylamines with amide substitution are capable of self-assembly into nanoarchitectures like rods (63, 64), fibers(65-68), and spheres (69, 70), and 2) crown-ethers can recognize ions selectively(71-77), crown-ethers were introduced into amide-substituted triarylamine backbones to form columnar synthetic ion channels (Figure 6a, compound **5A**)(62). The compound **5A** was successfully demonstrated as cation channels but failed to mediate water conduction. Instead, compound **6A** was synthesized to contain free carboxylic acids, which could interact with water molecules through H bonds. As a result, when the compound **6A** were reconstituted into lipid bilayers, it showed ~25% enhanced water permeability over **5A**, implying compounds **6A** could mediate water molecule translocation.

To rationlize these proposed phenomena, the crystal structures of compound **5B** and **6B** were invoked as structural analogues since compound **5A** and **6A** itself could not be crystallized (Figure 6c).These structures systemically indicated that, in all cases, triarylamine backbones act as core stacking materials to construct columnar structures, which agrees withprevious reports of triarylamine based nanoarchitectures. It was hypothesized that triarylamines with free carboxylic acid and long alkyl chains (compound **6A**) could be stacked into two-dimensional matrices, providing preferred pathways for water molecules to diffuse across the lipid bilayers. However, detailed studies are required to specifically determine the water transport properties of triarylamine-based synthetic water channels.

2.2. Unimolecular transmembrane channels

2.2.1. Pillar-arene based synthetic water channels

Recent progress in a new class of cyclic macromolecules, pillararenes, has opened a new chapter in the area of artificial water channels with the introduction of single molecule (or unimolecular) transmembrane channels(21, 22, 78-81). Distinctive characteristics of pillararenes, which have hollow-pillar shapes and feasibility of chemical modifications based on versatile aromatic hydroxyl groups, have inspired supramolecular chemists to synthesize channel-like tubular architectures with high aspect ratios and restricted pore sizes by extending side chains on pillararene templates. This intuitive strategy has been demonstrated as a promising candidate in designing efficient single molecular water channel systems (22).

Hydrazide-appended pillar[5]arene

Hydrazide-appended pillar[5]arenes (HAPs)were the first successful unimolecular artificial water channels, proposed by Hou and coworkers (81).The first evidence of HAP acting as water channels was the fact that a continuous 1D water wire could beformed inside the

pillar[5]arene derivative**7A**(Figure 7a) (80, 82). Enlightened by this observation, a series of hydrazide chain appended pillar[5]arenes were prepared (Figure 7b). Each structure was clearly defined as having intramolecular hydrogen bonds between hydrazide side chains, forming intact tubular structures. Interestingly, the crystal structure of **7B** revealed that the water wires are truncated at the middle of channels due to adjacent H bond donors coming from hydrazide backbones (Figure 7c).Consequently, since the continuous water wire is a key requirement for proton diffusion (28), HAP was expected to completely reject proton diffusion. This was subsequently demonstrated by experiments and the mechanism is found to be similar to that in AQP water channels (13, 83). From this point of view, the HAP channel can be regarded as first mimic of AQPs, which demonstrates aquaporin's water conduction (though the rate is orders of magnitude lower) while excluding protons in an artificial system. Nonetheless, the repeating hydrophilic hydrazide groups significantly hindered efficient water permeability of HAP channel due to hydrophilic interactions between water molecules and channel'sinner surfaces. The single channel water permeability was estimated as approximately 40 H_2O molecules/s/channel for channel structure **7C** whose length (5 nm) was reasonably matched with the thickness of lipid bilayers (~4nm) (22).

Peptide-appended pillar[5]arene

As a next version of pillar[5]arenebased artificial water channels,hydrophobic tripeptide chains of phenylalanine (Phe) isomers were introduced on pillar[5]arene backbones and termed peptide-appended pillar[5]arene channels(PAP[5]). In this version, peptide chains were used as replacements of hydrazine chains in the original HAP channels (Figure 8a) (79, 81). The channel structure of PAP[5] was extensively examined by concentration-titrated H-NMR, two-dimensional correlation spectroscopy and rotating-frame Overhauser effect spectroscopy, and it was demonstrated that the entire structure can be stabilized by

intramolecular H bonds between peptide chains, similar to that in HAP channels. In addition, all the phenyl groups of peptide chains were shown to face outward towards the hydrophobic core of the lipid bilayer, enhancing the stability of channels within hydrophobic bilayer regions. Molecular transport studies of PAP[5] channels in lipid membranes was conducted by Shen *et al* .through experiments and molecular dynamics (MD) simulations (21). PAP[5] was shown to have a single channel permeability of 3.5 $\times 10^8$ H_2Omolecules/s/channel which is in the range of aquaporins ($3.4 – 40.3 \times 10^8$ for AQP0 and AQP1 proteins, respectively at the two ends of the range), suggesting continuous and efficient water wire formation along withinthe inner environment of the channels. Together with these experimental results, MD simulations provided an understanding of molecular transport within the PAP[5] channel. Interestingly, during water diffusion, as observed in MD simulations, the channel pores suffered from wetting-dewetting transitions due to dynamic fluctuations of peptide chains, preventing continuous water diffusion over extended periods of time. Nonetheless, PAP[5] is known to have highest demonstrated single channel water permeability among artificial channel systems except for carbon nanotube porins (CNTPs) (84). However, PAP[5] showed compromised selectivity compared to the other systems. For example, even though PAP[5] showed the ion selective trend of Cl^-< Li^+< Na^+< K^+<Rb^+< Cs^+< NH_4^+which is corresponding with the Eisenman sequence I, the molecular weight cut-off was determined to be ~420 Da. This is attributed to the pore size of pillar[5]arene(~ 5Å)with an excellent agreement with a previous hypothesis that 3Å is critical pore diameter for efficient ion rejection(19).

2.2.2. Carbon nanotube porins

Hagen-Poiseuille flow is the classical model of Newtonian fluid flow, which is generally represented by water, flowing through long cylindrical pipe. This model has also provided a rationale for understanding transport behavior of such fluids flowing through porous

membranes but does not explain transport properties of nanometer or Angstrom scale flows (85, 86). In early 2000s, it was reported that water molecules can flow orders of magnitude faster inside hydrophobic nanotubes than that calculated from the Hagen-Poiseuille flow model (87-90). Since then, carbon nanotubes have been steadily highlighted as next generation materials for energy efficient water purification (88, 91-93). Recently,narrow 8Å-diameter-carbon nanotube porins (nCNTPs) were found to have single porin water permeability of $2.27\pm0.47\times10^{10}$ H_2O molecules/s/channel (84). This is first demonstration of an artificial channel system exceeding the AQP-1 in terms of water permeability, which has been firmly regarded as criterion for ideal water channel systems (Figure 9a). Compared to nCNTPs, wider 15Å-diameter-carbon nanotube porins (wCNTPs) showed an order of magnitude reduced water permeability ($1.97 \pm 0.43 \times 10^9$ H_2O molecules/s/channel). This was explained by invoking the water molecule confinement effects of nCNTPs via MD simulations and corresponding experimental results. Contrary to wCNTPs in which water molecules exist as bulk state, nCNTPs can sterically confine them into single file water wires (Figure 9 b and c). Since bulk state water molecules typically have higher number of H bonds (3.9 on average) than single file water molecules (1.8 on average), less confined water resulted in a higher energy barrier for water transport. In addition, the entirely hydrophobic inner surface of nCNTPsenabled it to have about 6-fold increased water permeability than AQP-1, indicating that important directions for designing artificial water channels in the future should include; 1) hydrophobic inner surface and 2) single water wire formation.

3. SYNTHESIS ROUTES FOR ARTIFICIAL WATER CHANNELS

To fabricate practical channel based membranes, cost and process efficient artificial channel synthesis is required. However, due to the diversity and complexity of each artificial channel structure, no standardized synthetic method has been firmly established, even though it has

been several decades since the first artificial channel was reported (94). However,it is important to consider synthesis routes from the perspective of macro-scale membrane fabrication leading to desired routes with simple synthetic steps. A brief summary of synthesis techniques is provided in the supporting information. Overall, the synthesis of self-assembling channels are simpler and require less number of steps than unimolecular channels, which provide other advantages in terms of stability and processibility.

4. IDEAL DESIGN OF WATER CHANNELS

Artificial water channels should ideally have high permeability for water while providing selective removal of targeted Angstrom-sized solutes. In this section we discuss properties that can be considered to be those of ideal water channels with removal of solutes primarily based on size. Inspiration and concepts for high performance artificial water channels are based on understanding of water transport in biological and current artificial water channels and the self-assembly behavior in various bilayer and bilayer-like matrices. The important properties for design of high performance artificial water channels are summarized in Figure 10 and current artificial channels are classified according to their performance in each category in Table 1.

Aquaporin like permeability

Since artificial water channels are inspired by aquaporins, the permeability of aquaporins of ~ 10^9 H_2O molecules/s/channel is an important benchmark for artificial channels to be compared against. It is thus important for channel characterization methods to obtain single channel permeability that is comparable to those that have been obtained for aquaporins and some artificial water channels (21, 95).

Usable cross-sectional area

A singular disadvantage of aquaporins in membrane materials is the low available usable cross-sectional area of aquaporins with a protein diameter of ~ 30 Å and a pore diameter of ~3 Å. Thus, even if aquaporins are packed tightly into two dimensional crystals in lipids or amphiphilic block copolymers (BCPs) with a unit cell size of ~ 95 x 95 Å square per tetramer, the effective porosity of such a membrane is still only ~0.3% (96). Artificial channels that have a high usable cross-sectional area thus provide an opportunity to take advantage of the high permeability properties inspired by AQPs but avoid its disadvantage of low effective cross-sectional area.

Hydrophobic outer surfaces

Artificial water channels are, in general, designed to be inserted in lipid bilayer membranes or their synthetic polymer analogs, amphiphilic BCP membranes. Thus, for stable insertion into such membranes, the outer surface of these channels has to be compatible with the hydrophobic interior or core of the lipid bilayer or the hydrophobic block of the BCP used. While just being hydrophobic has been considered to be sufficient in the past, the increasing variety of membrane substrates has focused attention on the hydrophobic chemical compatibility between the membrane facing surface of both biological and artificial channels and the hydrophobic core of the membrane (97). We propose that the hydrophobicity of the membrane-facing surface of the channel should be similar in hydrophobicity to the molecules forming the hydrophobic core of the membrane and have developed a fluorescence based assay to test this compatibility (97). However, a predictive understanding of such compatibility based on known compositions of the outer surface of channels and membranes is still lacking and a need in the field of artificial water channels specifically and channel-based biomimetic and bioinspired membranes in general.

Hydrophobic interior surfaces

It has become increasingly clear that, in confined nanometer scale channels, permeability is enhanced orders of magnitude over Hagen-Poiseuille flow in smooth hydrophobic pores such as in carbon nanotubes (88, 91, 98). This enhancement has been attributed, among other reasons, to the slip flow that is possible in such systems. Recently, Peter Pohl and coworkers have described a unified correlation that describes increase in diffusivity of water in biological and artificial channels with decreasing number of hydrogen bonds between the pore wall and the confined water wire (98). Therefore, we propose that, for the ideal water channel, the interior surface should be smooth and hydrophobic, with little or no interaction with the water wire.

Hydrophilic channel entrances

While the exterior and the interior "wall" of artificial water channels should be hydrophobic to increase compatibility with bilayer like structures for enhanced transport, having hydrophobic ends on the water channels may provide an energy barrier for entrance of water molecules into the channel. As suggested for carbon nanotubes and as seen in biological channels, we propose that the ends of artificial channels be functionalized with hydrophilic molecules to reduce the barrier to water entry (84) and to enhance compatibility with the hydrophilic outer regions of biomimetic membranes composed of lipids with hydrophobic head groups and BCPs with hydrophilic end blocks.

Length matching of channels with membrane thickness

Physical matching of the length of membrane proteins with the thickness of the bilayer has been discussed as being critical to both membrane protein function and its stable insertion in such membranes (97, 99). We propose that the lengths of artificial channel be designed so that its hydrophobic length matches the hydrophobic thickness of the membrane and its overall length match the overall thickness of the membrane.

Structural rigidity

It is important for artificial water channels to maximize their open probability (the fraction of time it remains open) in order to achieve desired performance. In the case of PAP[5] channels it has been observed that the peptide arms forming the channel walls at the entrance and exit of the channel are dynamic floppy and can sometimes assume a conformation that occludes the pore, leading to a reduction in overall time averaged permeability (Figure 8c) (21). We propose that rigid channels that are less dynamic may be a property that can be important for ideal artificial water channels.

Unimolecular vs. Self-assembled channels

Unimolecular channels provide several advantages compared to self-assembled channels when the ease of creating high performance membranes around artificial water channels is considered. The primary advantage is the ability to maintain a channel configuration regardless of small changes in the properties of the membrane matrix. Self-assembled channels also have the challenge of making transitory pores reducing the amount of time available for water and solute transport. Additionally, self-assembled channels have not been shown to be active in materials beyond lipid bilayers while some unimolecular channels have been recently demonstrated in BCPs (100).

5. DESIGN CONSIDERATIONS FOR MEMBRANE FABRICATION AROUND ARTIFICIAL WATER CHANNELS

The ultimate goal of designing artificial water channels is to incorporate them into macroscale membranes for applications in aqueous separations. Thus, design of such membranes should enable the high selectivity and permeability observed in molecular transport to be translated to the resulting membrane while providing a stable material that can withstand operating conditions such as high pressure. The following subsections describe

desirable properties of membrane materials that are based on artificial water channels, and then describe three hypothetical designs based on a current understanding of these materials and requirements for current solute separation membranes

5.1 Desired properties in artificial channel membranes

High packing of channels

A current disadvantage of biomimetic membranes based on AQPs is the low density of water channels per unit area of ~ 30-40 channels/μm^2(21). Further even if the number of channels is improved to its theoretical maximum by creating 2D crystals of these membrane proteins, the usable pore area is still <1% of the total area due to the small pore size to total protein cross sectional area in aquaporins. Artificial channels in general have a much higher usable cross-sectional area then membrane proteins (21).However, to take advantage of this feature, they must be tightly packed into membranes to provide the maximum permeability possible from these membranes.

High rigidity and mechanical toughness

Most solute separation membranes such as ROmembranes operate under high pressures from 5-70 bars. Thus, high rigidity and physical toughness is an important requirement for such membranes. The Young's Modulus of RO active layer polyamide is ~ 1 GPa and its fracture strength is ~ 66 MPa (101).We propose that similar properties would be necessary for materials based on artificial channels for solute separation membrane applications based on highly crosslinked layers in which channels are incorporated.

Highly aligned channels

Highly aligned channels are important for the permeability properties of membranes created from artificial water channels as unaligned channels will not be productive and lead to low

permeability areas on membrane surfaces. Lack of alignment or low alignment has been a persistent challenge with carbon nanotube membranes (102, 103). The architecture of most artificial channels that have evolved from testing in self assembled lipid based systems which allows for spontaneous alignment of channels within the bilayer environment provides an advantage as far as alignment is considered within self-assembled lipid and lipid like BCP membranes.

Low prevalence of defects

A large challenge to creating membranes around designer small molecules and assemblies such as zeolites and MOFs is their defect-free integration into polymeric substrates (104, 105). The presence of pinholes and other defects are highly detrimental to the selectivity of membranes, particularly when the target separation is in the sub nanometer scale. This is perhaps the largest challenge in creating scalable membranes using artificial water channels at the present time.

5.2. Three possible designs for artificial water channel membrane fabrication

Artificial water channel based membrane research is in an early stage of development. Most membrane transport properties have only been characterized using small membrane vesicles of sizes ~200 nm in diameter. On the other hand, work on the synthesis of AQP based desalination membrane has seen substantial progress in the past few years (11). Based on this progress we suggest that artificial water channels would be used to develop practical membrane fabrication utilizing concepts similar to that for AQP-based membranes. Additionally, other more scalable concepts that utilize the solvent stability of artificial water channels could be employed. The following subsections describe our view of three strategies that seem feasible for creating macroscale membranes based on artificial water channels.

5.2.1. Membranes based on incorporation of channel-rich vesicles into selective layers of current membranes

Current water desalination reverse osmosi (RO) membranes have structures that are comprised of a porous support membrane with a thin selective layer on the top (5, 11, 106, 107). The most tested AQP-based membrane designs have focused on embedding, adsorbing or grafting functional AQP-incorporated vesicles into or onto the selective layers of membranes (including RO membranes) so that AQPs can provide energy efficient passageways for water molecules across the membrane. To achieve practical selective layers, various methods have been utilized including pressure driven vesicle fusion(108-112), polyelectrolyte adsorption (108, 113, 114), magnetically induced adsorption(114), chemical cross-linking (109-112, 115, 116) and proteoliposome incorporation into thin film composite RO membranes via interfacial polymerization (117).Of these techniques, proteoliposome incorporation into RO membrane active layers has resulted in a commercial product in both flat sheet and hollow fiber forms (118). These membranes showed substantial permeability improvements maintaining promising selectivity compared to commercial RO or nanofiltration (NF) membranes, even though several questions still remain regarding the long-standing stability of protein water channels against high hydraulic operating pressure, salinity, fouling effects and microbes (11).On the other hand, in synthetic water channel systems, it may be possible to minimize these possible disadvantages of biological and possible mechanical instability while maintaining the merits of using water channels (21). We propose designs parallel to those utilized for AQPs as possible designs for artificial channel-based membranes (Figure 11)

5.2.2. Layered deposition of two-dimensional channel embedded nanosheets

To maximize the advantages of exploiting biological and artificial water channels in

membrane fabrication, our group has proposed using highly porous 2D nanosheet-based membranes which are composed of water channels and amphiphilic molecules (lipids or BCPs)(Figure 12 aandc)(21, 119-121). 2D nanosheets and crystal assembly in lipids and BCPs has been shown to be possible for various protein channels as well as unimolecular artificial water channels including AQPs, outer membrane protein F (OmpF), and PAP[5](21, 119-121). The structural features of these nanosheet membranes are similar to channel-incorporated vesicles but they have significantly higher molar ratios of channels to amphiphilic molecules (~ 0.8) than those of conventionally reconstituted vesicles (~0.001 to 0.002) and they are flat sheets rather than hollow spheres. These crystalized (or highly ordered array) structures have highly organized water channels with high pore density per unit area of up to 10^5 channels/μm^2(21). Also, these 2D crystalline structures could be as large as several microns size with high aspect ratios of ~1000. Together with two considerations of high pore density and scalability, nanosheet membranes can be regarded as promising materials for practical selective layer formation for water treatment or small molecule separation membranes.

Recently, we have successfully demonstrated that artificial water channel embedded nanosheets, which are made of PAP[5] and polybutadiene-polyethylene oxide (PB-PEO)diblockBCPs, could be used to form continuous and scalable selective layer on the top of track-etched polycarbonate (PC) or polyethersulfone (PES) membranesby simple pressure-driven lateral deposition(100).For these kind of soft materials, achieving sufficient mechanical stability against substantial hydraulic pressure has been one of the most challenging problems for practical membrane applications. However, due to the feasibility of BCPs with respect to chemical modification, another supporting polymeric layer of polyethyleneimine (PEI) could be introduced and then chemically cross-linked with each

nanosheet layers to confer higher stability to thin selective layers by forming layer by layer structures (Figure 12).

5.2.3. Lamellar structured BCP membrane

Distinctive phase segregation behaviors of BCPs have led to their investigation and application into various research and industrial fields (122-124). They have been well characterized as having unique patterning (self-assembling) properties, depending on volume fractions of blocksand the difference in their hydrophobicity to develop unique polymer structures(122). For example, amphiphilic diblockBCPs can self-assemble into cubic spheres, hexagonal cylinders, bicontinuous gyroids and lamellae below the order−disorder transition temperature, depending on volume fractions (Figure 13a).Since these domain separations can be carried out at micro or nanometer scale with regular patterns, they are being extensively used as templates in nanolithography, nanoparticle synthesis and isoporous nanopore membrane fabrication(125-127).

Among these various patterns of BCPs, the lamellar structure could be of high interest in terms of efficient biomimetic membrane fabrication around artificial channels. Also, since the water channels have been demonstrated to be functional in BCP bilayer membranes(120, 121), BCPs can be considered as next generational materials for practical biomimetic membrane development, due to their low cost, rich functionality and robustness(123, 124). In this context, incorporation of artificial water channels into lamellar structured BCP matrix, which can provide similar environments of cellular membranes for biomimetic channels,can be a reasonable approach to developing synthetic biomimetic membrane systems (Figure 13). Under these circumstances, the artificial channels can be selectively inserted into the hydrophobic phases in a direction perpendicular to the lamellar plane. The transport property of the membranes would then be critically determined by channel’s water conduction and

selective properties (Figure 13c and d).

6. OUTLOOK FOR ARTIFICIAL CHANNEL BASED MEMBRANES

Artificial water channels are promising alternatives to aquaporins for membrane-based, energy efficient Angstrom-scale separations. These are expected to overcome or at least minimize several disadvantages of AQP-based biomimetic membranes that originate from their intrinsic properties of being biomaterials (proteins) including cost efficiency and mechanical and chemical stability against non-homeostatic environments, from the materials engineering and operation perspectives. Even though current artificial channels systems are still in early stages of development, there has been remarkable progress in the past five years, particularly in molecular design and demonstration of synthetic channels with performance comparable to AQPs, suggesting a promising future for research, development and commercialization in this area. Further, recent advancements in nanomanufacturing technologies could greatly enhance the possibility of developing practical membrane fabrication schemes using artificial water channel systems in the near future.

DISCLOSURE STATEMENT

The authors are not aware of any affiliations, memberships, funding, or financial holdings that might be perceived as affecting the objectivity of this review.

ACKNOWLEDGEMENTS

The authors acknowledge financial support from the National Science Foundation CAREER grant (CBET-1552571) to MK for this work. Support was also provided through CBET-1705278 and DMR- 1709522 for various aspects of this work.

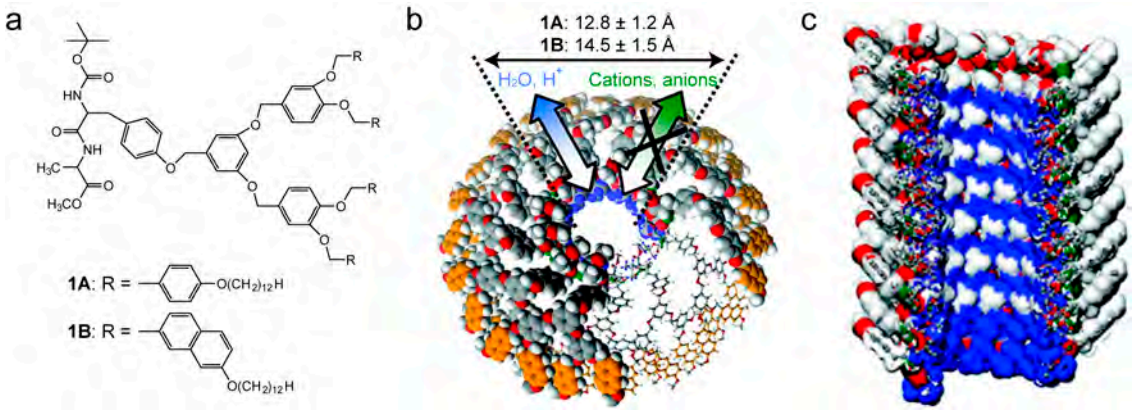

Figure1. Dendritic dipeptide pores. (a) Chemical structures of dendritic dipeptideswith different dendritic periphery arms. (b) Top and (c) cross-sectional views of simulationmodel of dendritic hydrophobic pores. Dendritic periphery arms were not shown in (c). Reprinted with permission from Reference (24). Copyright © 2007, American Chemical Society.

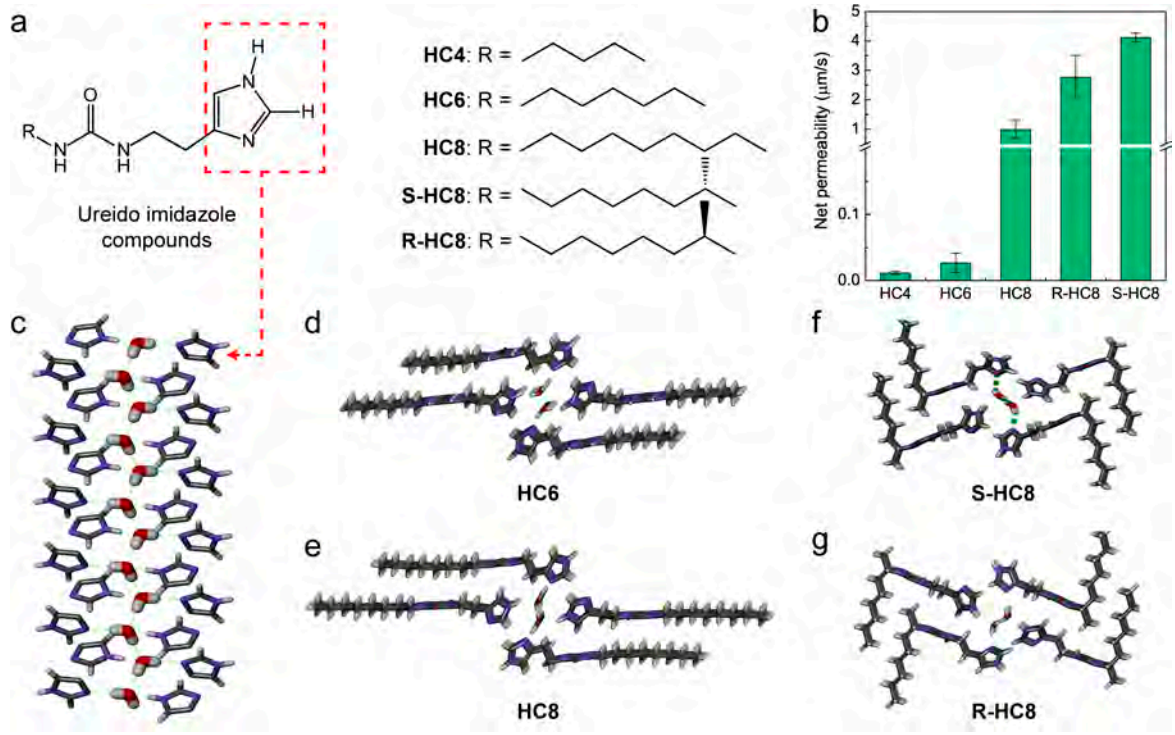

Figure 2. I-quartet channels. (a) Chemical structures of ureido imidazole compounds with various alkyl chain tails in terms of chain length and chilarity. (b) I-quartet channel embedded vesicular membrane water permeabilities. (c) Columnar assembly of imidazole moieites inside hydrophobic environments. Hydrated crystal structures of (d) **HC6**, (e) **HC8**, (f) **S-HC8** and (g) **R-HC8** which are containing dipolar water wires.Reprinted with permission from Reference (19). Copyright © 2016, American Chemical Society.

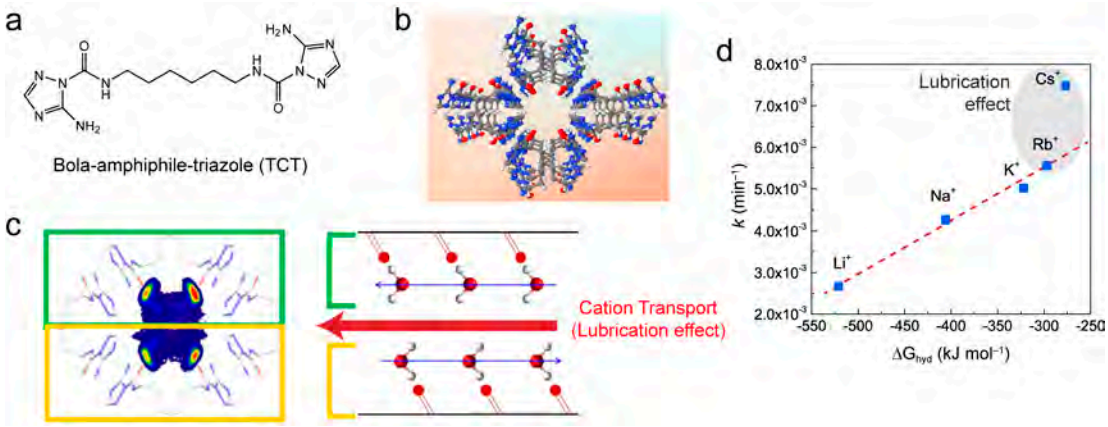

Figure 3. Triazole channels (T-channels). (a) Chemical structure of bola-amphiphile-triazole TCT. (b) Single columnar crystal structure of T-channels. (c) Water-filled model of T-channels. Half of four water wires (upper green box) are facing opposite directions with respect to another half of water wires (below yellow box). These water wires hydrate the inner surface of water channels and reduce direct interactions between small cations and water channels, resulting in lubricant effect for small cation transport. (d) Anomalous single order exponential behavior of cation transport activities of T-channels. Dashed red line represents conventional linear trend of Eisenman I cation conduction rates.Reprinted with permission from Reference(35). Copyright © 2014, Nature Publishing Group.

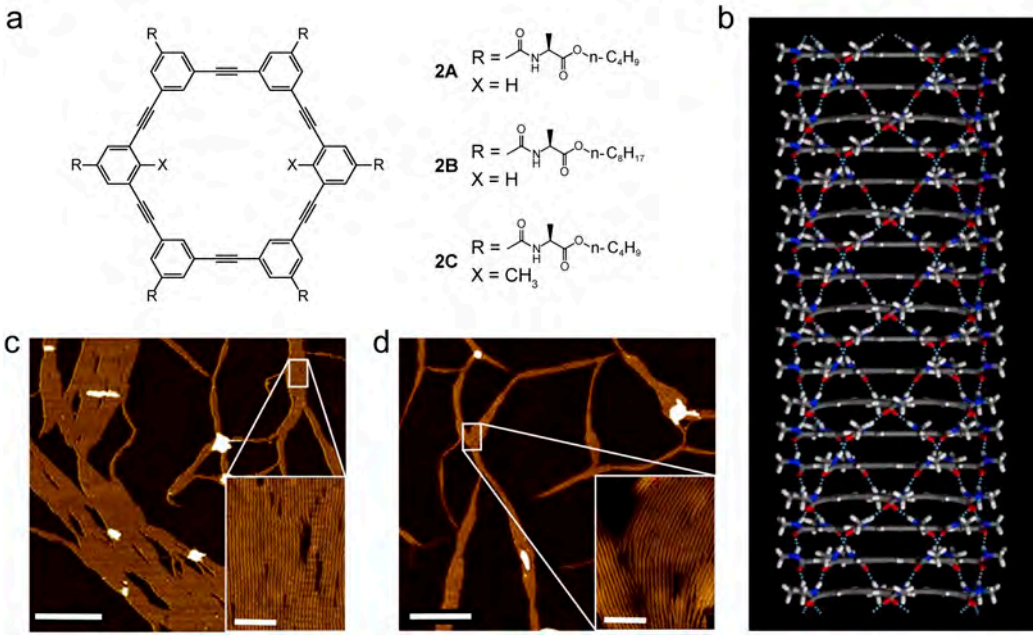

Figure 4.*m*-PE channels. (a) Chemical structures of hexa(*m*-PE) based planar macrocycles.(b) A snap shot of quantum molecular dynamic simulations for stacked columnar pore structure of **2A**. Atomic force microscopy (AFM) images of assembled pillar structures of (c) **2A** and (d) **2B**on the mica substrate in CCl_4. Scale barsare 500 nm for main figures and 50 nm for insets.Reprinted with permission from Reference(42). Copyright © 2012, Nature Publishing Group.

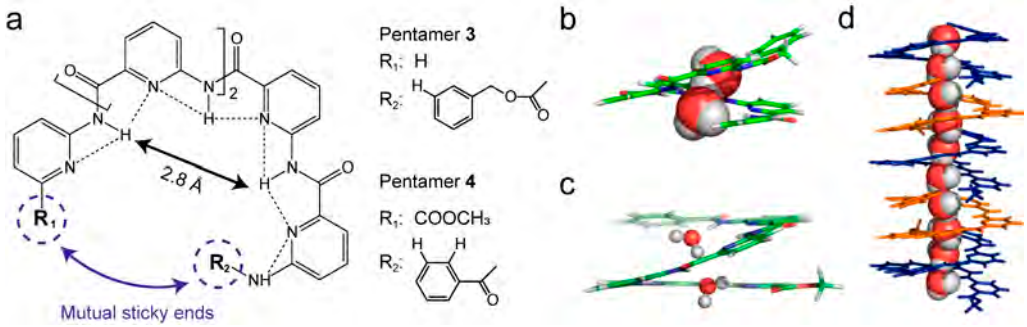

Figure 5. Aquafoldamers. (a) Chemical structure of folding pentamers with different pairs of sticky ends. Hydrated crystal structures of (b) pentamer **3** and (c) pentamer **4** which are containing two water molecules per repeating unit. (d) 1D water wire containing helical aquapore consists of pentamer **4** which are self-elongated by sticky ends.Reprinted with permission from Reference(60). Copyright © 2014, American Chemical Society.

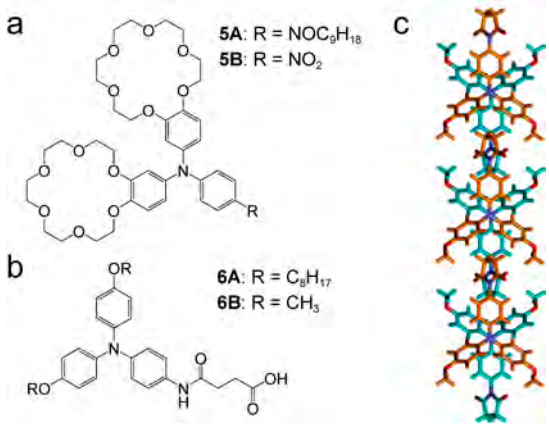

Figure 6. Triarylamine channels. Chemical compositions of triarylamine monomers for synthetic (a) cation and (b) water channels.(c) Crystal structure of **6B**.Reprinted with permission from Reference(62). Copyright © 2017, American Chemical Society.

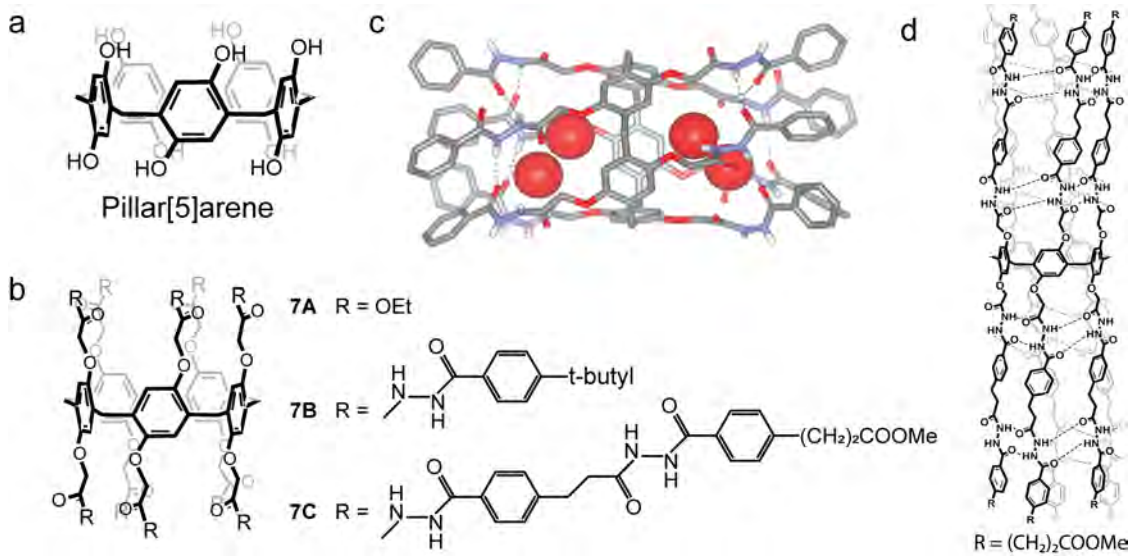

Figure7. Hydrazide-appended pillar[5]arenes (PAH). (a) Crystal structure of pillar[5]arene. (b) A series of hydrazide chain extended pillar[5]arenes. (c) Chemical structure of **7B** which contains a truncated water wire in the middle of the channel. O atom of water molecules are represented by space-filling (CPK) model. (d) Schematic tubular conformation of **7C**.Reprinted with permission from Reference (99). Copyright © 2012, American Chemical Society.

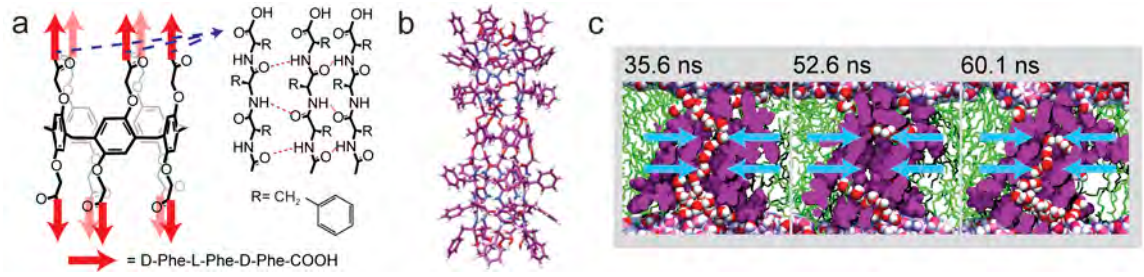

Figure 8. Peptide-appended pillar[5]arene (PAP[5]). (a) Schematic illustration of PAP[5] chemical structure. (b) Molecular modeling of PAP[5] channel. (c) Snap shots of MD simulation showing wetting-dewetting transition of PAP[5] channel. Channels are represented by purple van der Waals spheres. 1-palmitoyl-2-oleoyl-*sn*-glycerol-3-phosphatidylcholine (POPC) lipids are used as bilayer matrix and represented by green stick model. Water molecules are represented by red and white van der Waals spheres.Reprinted with permission from Reference(21). Copyright © 2015, National Academy of Sciences.

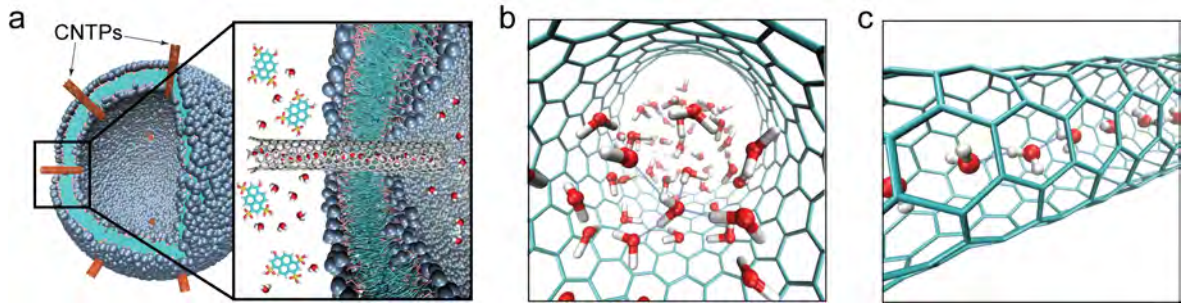

Figure 9. Carbon nanotube porins (CNTPs). (a) Illustration of CNTP mediated water conductionacross lipid bilayers.Snap shots of MD simulations which are showing the status of water molecules as (b) bulk or (c) single file inside the wCNTPornCNTP respectively.Reprinted with permission from Reference(84). Copyright © 2017, The American Association for the Advancement of Science.

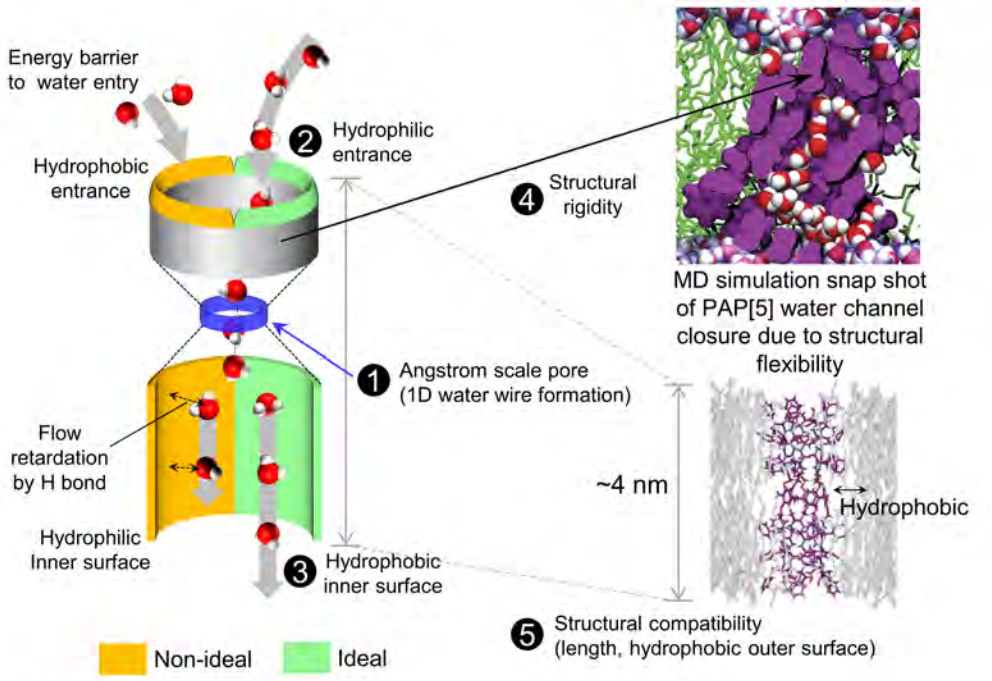

Figure 10. Ideal water channel design considerations.(1) Rigid pore structure at Angstrom scale for selective and fast water diffusionby 1D water wire formation. (2) Hydrophilic channel entrance to reduce unfavorable energy barrier to water molecule entry into the channel. (3) Hydrophobic inner surface to minimize any interaction between water molecules and channel interface which can result in flow retardation. (4) Rigid structural stability to prevent dynamic deformation of channel structure which can hinder continuous water conduction. (5) Structural compability of water channels against biomietic membrane matrix in terms of length and hydrophobic compatibility. Parts of the figure reprinted with permission from Reference (21). Copyright © 2015, National Academy of Sciences.

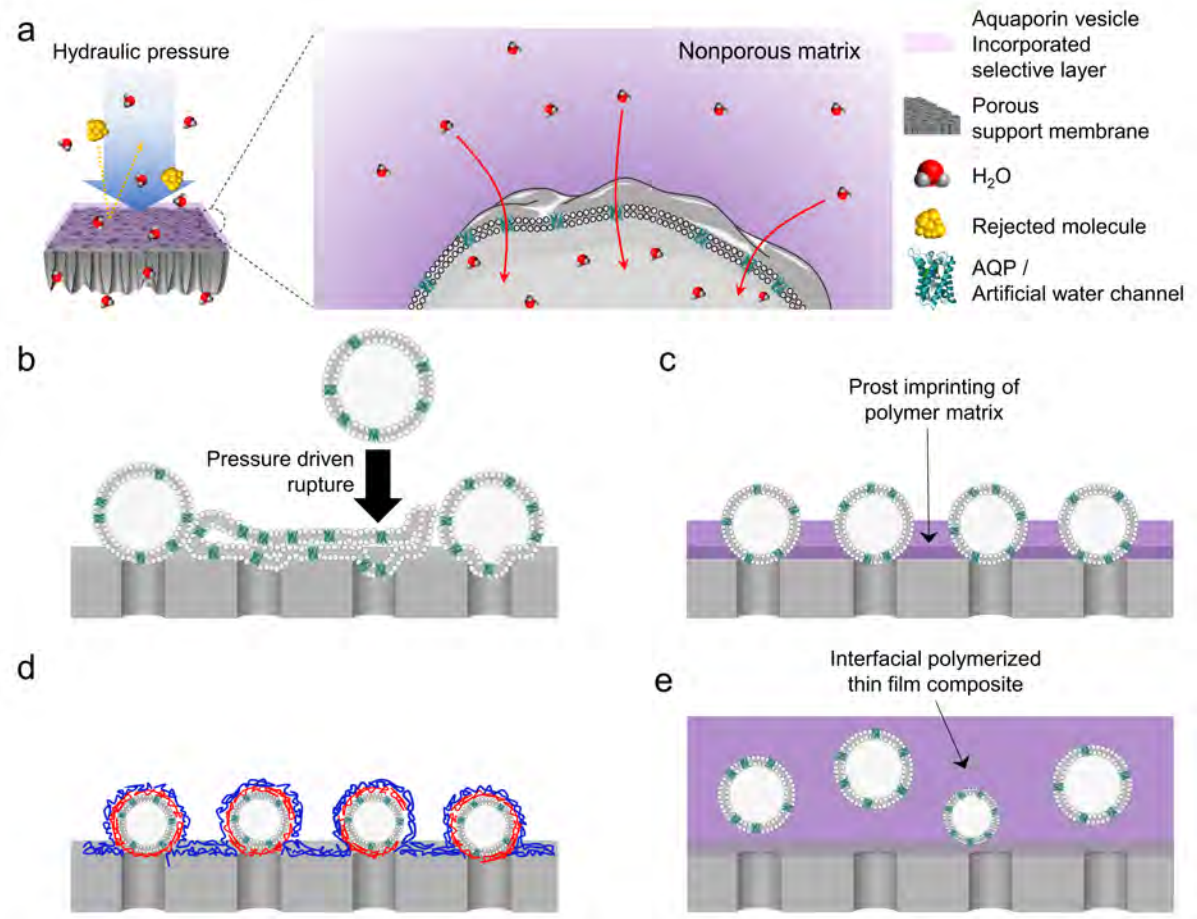

Figure 11. Schematic illustrations of several strategies to fabricate water channel based desalination membranes based on current efforts with AQP-based vesicles. (a) Overview of current water channel vesicle incorporated desalination membranes that could be adapted for artificial channel based macro scale membranes. (b) Pressure driven vesicle rupture, (c) imprinting of vesicles, (d) polyelectrolytic adsorption of vesicles and (e) vesicle embedment into thin film composite via interfacial polymerization. Part of figure reprinted with permission from Reference(107). Copyright © 2012, Elsevier.

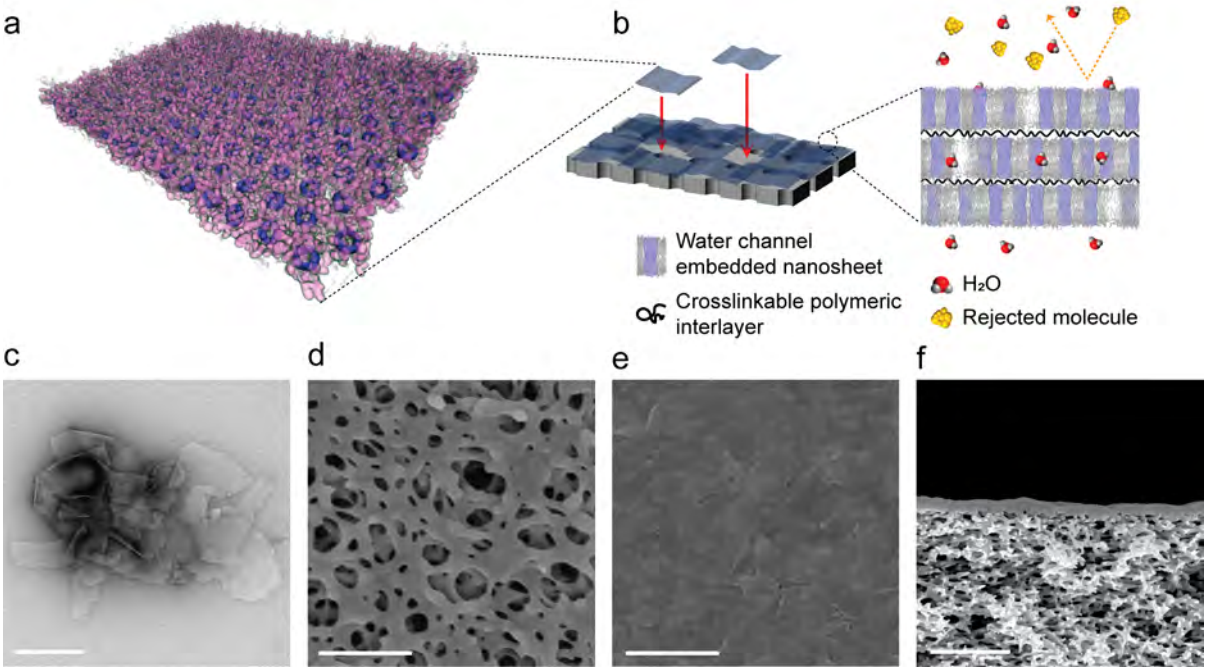

Figure 12. Layered deposition of channel embedded 2D nanosheets on porous support membrane. (a) Tilted view of molecular modeling of hexagonally ordered PAP[5] 2D nanosheet. Narrowest pore regions of PAP[5] are presented as dark violet. Peptide phenylalanine arms are presented as translucent purple. Lipid bilayers are presented as translucent gray polygons. (b) Schematic illustration for layered deposition of artificial water channel embedded nanosheets on porous support. (c) Transmission electron microscopy (TEM) image of channel protein (OmpF) embedded nanosheets. Scale bar is 500 nm. Scanning electron microscopy (SEM) images (d) before and (e) after artificial water channel embedded nanosheets deposition on the PES support. Scale bars are 1μm. (f) Cross-sectional SEM image of deposited selective layer of nanosheets on the PES support. Scale bar is 2μm. Reprinted with permission from Reference (21). Copyright © 2015, National Academy of Sciences.

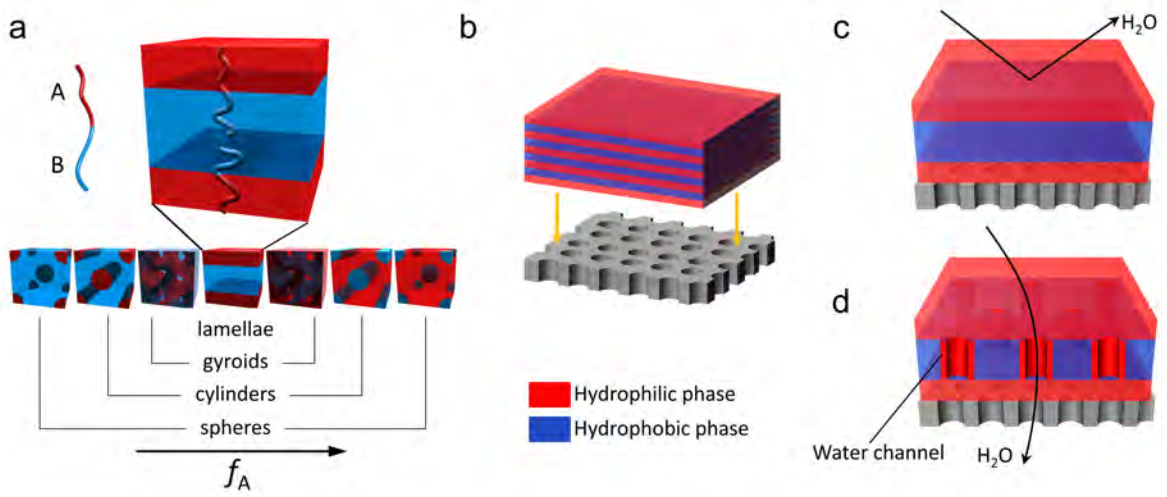

Figure 13. Suggested design for lamellar BCPartificial water channel membrane. (a) Phase separation properties of diblockBCPs depending on volume fraction of A (f_A) and the difference in hydrophobicity between the two blocks. (b) Schematic illustration for preparation of lamellar structured selective layer on porous support. Anticipated water transport phenomena across the lamellar selective layer (c) before and (d) after water channel incorporation into hydrophobic phases. Panel (a) reprinted with permission from Reference (122). Copyright © 2007, Elsevier.

Table 1. Ideal water channel considerations for current artificial water channels.

Channels	Classification	Single channel permeability (H_2O / s)	Pore diameter (Å)	Hydrophilic entrance	H bond with water wire (number)	Usable crosssectional area (%)	Structural rigidity	Length matching difference[a]
Dendritic dipeptide	Self-assembled	NA	~14.5	No	NA	3	Thermally unstable (T_m = 40°C)	~1
I-quartet		**HC8** : 1.4 X 10^6 **R-HC8** : 7.9X 10^5 **S-HC8** : 1.5X 10^6	~2.6	Yes	Yes (4)[b]	5 - 10[c]	Dynamic	
Triazole		NA	~5 (average)	Yes	Yes (4)[b]	~20[c]	NA	
m-PE		NA	~6.4	No	None	4	Rigid	
Aquafoldamer		NA	~2.8	Yes	Yes (5)[b]	10 - 15[c]	NA	
Triarylamine		NA	NA	Yes	NA	NA	NA	
HAP	Unimolecular	**6D** :40	~4.7	Yes	Yes(90)[d]	20 - 25[c]	Pore :rigid Wall : dynamic	**6A** : 0.4 **6B** : 0.875 **6D** : 1.25
PAP[5]		3.5 X 10^8	~4.7	Yes	None	20 – 25[c]	Pore :rigid Wall : dynamic	0.8
CNTPs		nCNTP : 2.8 X 10^{10} wCNTP : 2 X 10^9	nCNTP : 8 wCNTP : 15	Yes (modification)	None	~100	Rigid	2.5

[a] Ratio of water channel length to height of lipid bilayer.

[b] Number of H bonds per repeating assembly unit of crystal structure

[c] These are calculated approximately based on top view of water channel crystal structures.

[d] Number of potential H bond acceptor around inner surface of single water channel

LETERATURE CITED

1. Imbrogno J, Belfort G. 2016. Membrane Desalination: Where Are We, and What Can We Learn from Fundamentals? *Annual Review of Chemical and Biomolecular Engineering* 7: 29-64
2. Marchetti P, Jimenez Solomon MF, Szekely G, Livingston AG. 2014. Molecular Separation with Organic Solvent Nanofiltration: A Critical Review. *Chemical Reviews* 114: 10735-806
3. Baker RW. 2010. Research needs in the membrane separation industry: Looking back, looking forward. *Journal of Membrane Science* 362: 134-36
4. Kumar P, Sharma N, Ranjan R, Kumar S, Bhat ZF, Jeong DK. 2013. Perspective of Membrane Technology in Dairy Industry: A Review. *Asian-Australasian Journal of Animal Sciences* 26: 1347-58
5. Park HB, Kamcev J, Robeson LM, Elimelech M, Freeman BD. 2017. Maximizing the right stuff: The trade-off between membrane permeability and selectivity. *Science* 356
6. Bernardo P, Drioli E, Golemme G. 2009. Membrane Gas Separation: A Review/State of the Art. *Industrial & Engineering Chemistry Research* 48: 4638-63
7. Le NL, Nunes SP. 2016. Materials and membrane technologies for water and energy sustainability. *Sustainable Materials and Technologies* 7: 1-28
8. Shannon MA, Bohn PW, Elimelech M, Georgiadis JG, Mariñas BJ, Mayes AM. 2008. Science and technology for water purification in the coming decades. *Nature* 452: 301
9. Khawaji AD, Kutubkhanah IK, Wie J-M. 2008. Advances in seawater desalination technologies. *Desalination* 221: 47-69
10. Freeman BD. 1999. Basis of Permeability/Selectivity Tradeoff Relations in Polymeric Gas Separation Membranes. *Macromolecules* 32: 375-80
11. Shen Y-x, Saboe PO, Sines IT, Erbakan M, Kumar M. 2014. Biomimetic membranes: A review. *Journal of Membrane Science* 454: 359-81
12. Agre P, Bonhivers M, Borgnia MJ. 1998. The Aquaporins, Blueprints for Cellular Plumbing Systems. *Journal of Biological Chemistry* 273: 14659-62
13. Tajkhorshid E, Nollert P, Jensen MØ, Miercke LJW, O'Connell J, et al. 2002. Control of the Selectivity of the Aquaporin Water Channel Family by Global Orientational Tuning. *Science* 296: 525-30
14. Murata K, Mitsuoka K, Hirai T, Walz T, Agre P, et al. 2000. Structural determinants of water permeation through aquaporin-1. *Nature* 407: 599
15. Werber JR, Osuji CO, Elimelech M. 2016. Materials for next-generation desalination and water purification membranes. *Nature Reviews Materials*: 16018
16. Barboiu M. 2016. Artificial water channels - incipient innovative developments. *Chemical Communications* 52: 5657-65
17. Barboiu M. 2012. Artificial Water Channels. *Angewandte Chemie International Edition* 51: 11674-76
18. Zhou X, Liu G, Yamato K, Shen Y, Cheng R, et al. 2012. Self-assembling subnanometer pores with unusual mass-transport properties. *Nat Commun* 3: 949
19. Licsandru E, Kocsis I, Shen Y-x, Murail S, Legrand Y-M, et al. 2016. Salt-Excluding Artificial Water Channels Exhibiting Enhanced Dipolar Water and Proton Translocation. *Journal of the American Chemical Society*
20. Schneider S, Licsandru E-D, Kocsis I, Gilles A, Dumitru F, et al. 2017. Columnar Self-Assemblies of Triarylamines as Scaffolds for Artificial Biomimetic Channels for Ion and for Water Transport. *Journal of the American Chemical Society*
21. Shen YX, Si W, Erbakan M, Decker K, De Zorzi R, et al. 2015. Highly permeable artificial water channels that can self-assemble into two-dimensional arrays. *Proc Natl Acad Sci U S A* 112: 9810-5
22. Si W, Xin P, Li ZT, Hou JL. 2015. Tubular Unimolecular Transmembrane Channels:

Construction Strategy and Transport Activities. *Acc Chem Res* 48: 1612-9
23. Percec V, Dulcey AE, Balagurusamy VSK, Miura Y, Smidrkal J, et al. 2004. Self-assembly of amphiphilic dendritic dipeptides into helical pores. *Nature* 430: 764-68
24. Kaucher MS, Peterca M, Dulcey AE, Kim AJ, Vinogradov SA, et al. 2007. Selective Transport of Water Mediated by Porous Dendritic Dipeptides. *Journal of the American Chemical Society* 129: 11698-99
25. Roux B. 2002. Computational Studies of the Gramicidin Channel. *Accounts of Chemical Research* 35: 366-75
26. Burkhart BM, Li N, Langs DA, Pangborn WA, Duax WL. 1998. The conducting form of gramicidin A is a right-handed double-stranded double helix. *Proceedings of the National Academy of Sciences* 95: 12950-55
27. Allen TW, Andersen OS, Roux B. 2004. Energetics of ion conduction through the gramicidin channel. *Proceedings of the National Academy of Sciences* 101: 117-22
28. Agmon N. 1995. The Grotthuss mechanism. *Chemical Physics Letters* 244: 456-62
29. Schnell JR, Chou JJ. 2008. Structure and mechanism of the M2 proton channel of influenza A virus. *Nature* 451: 591
30. Stouffer AL, Acharya R, Salom D, Levine AS, Di Costanzo L, et al. 2008. Structural basis for the function and inhibition of an influenza virus proton channel. *Nature* 451: 596
31. Phongphanphanee S, Rungrotmongkol T, Yoshida N, Hannongbua S, Hirata F. 2010. Proton Transport through the Influenza A M2 Channel: Three-Dimensional Reference Interaction Site Model Study. *Journal of the American Chemical Society* 132: 9782-88
32. Hu F, Luo W, Hong M. 2010. Mechanisms of Proton Conduction and Gating in Influenza M2 Proton Channels from Solid-State NMR. *Science* 330: 505
33. Pinto LH, Dieckmann GR, Gandhi CS, Papworth CG, Braman J, et al. 1997. A functionally defined model for the M2 proton channel of influenza A virus suggests a mechanism for its ion selectivity. *Proceedings of the National Academy of Sciences* 94: 11301-06
34. Le Duc Y, Michau M, Gilles A, Gence V, Legrand Y-M, et al. 2011. Imidazole-Quartet Water and Proton Dipolar Channels. *Angewandte Chemie International Edition* 50: 11366-72
35. Barboiu M, Le Duc Y, Gilles A, Cazade P-A, Michau M, et al. 2014. An artificial primitive mimic of the Gramicidin-A channel. 5: 4142
36. Chui JKW, Fyles TM. 2012. Ionic conductance of synthetic channels: analysis, lessons, and recommendations. *Chemical Society Reviews* 41: 148-75
37. Bong DT, Clark TD, Granja JR, Ghadiri MR. 2001. Self-Assembling Organic Nanotubes. *Angewandte Chemie International Edition* 40: 988-1011
38. Moore JS, Zhang J. 1992. Efficient Synthesis of Nanoscale Macrocyclic Hydrocarbons. *Angewandte Chemie International Edition in English* 31: 922-24
39. Höger S, Bonrad K, Mourran A, Beginn U, Möller M. 2001. Synthesis, Aggregation, and Adsorption Phenomena of Shape-Persistent Macrocycles with Extraannular Polyalkyl Substituents. *Journal of the American Chemical Society* 123: 5651-59
40. Li X, Yang K, Su J, Guo H. 2014. Water transport through a transmembrane channel formed by arylene ethynylene macrocycles. *RSC Advances* 4: 3245-52
41. Gong B. 2008. Hollow Crescents, Helices, and Macrocycles from Enforced Folding and Folding-Assisted Macrocyclization. *Accounts of Chemical Research* 41: 1376-86
42. Zhou X, Liu G, Yamato K, Shen Y, Cheng R, et al. 2012. Self-assembling subnanometer pores with unusual mass-transport properties. 3: 949
43. Vijayvergiya V, Wilson R, Chorak A, Gao PF, Cross TA, Busath DD. 2004. Proton Conductance of Influenza Virus M2 Protein in Planar Lipid Bilayers. *Biophysical Journal* 87: 1697-704
44. Qin B, Sun C, Liu Y, Shen J, Ye R, et al. 2011. One-Pot Synthesis of Hybrid Macrocyclic Pentamers with Variable Functionalizations around the Periphery. *Organic Letters* 13: 2270-73

45. Yan Y, Qin B, Shu Y, Chen X, Yip YK, et al. 2009. Helical Organization in Foldable Aromatic Oligoamides by a Continuous Hydrogen-Bonding Network. *Organic Letters* 11: 1201-04
46. Yan Y, Qin B, Ren C, Chen X, Yip YK, et al. 2010. Synthesis, Structural Investigations, Hydrogen−Deuterium Exchange Studies, and Molecular Modeling of Conformationally Stablilized Aromatic Oligoamides. *Journal of the American Chemical Society* 132: 5869-79
47. Du Z, Ren C, Ye R, Shen J, Maurizot V, et al. 2011. BOP-mediated one-pot synthesis of C5-symmetric macrocyclic pyridone pentamers. *Chemical Communications* 47: 12488-90
48. Ren C, Maurizot V, Zhao H, Shen J, Zhou F, et al. 2011. Five-Fold-Symmetric Macrocyclic Aromatic Pentamers: High-Affinity Cation Recognition, Ion-Pair-Induced Columnar Stacking, and Nanofibrillation. *Journal of the American Chemical Society* 133: 13930-33
49. Ren C, Zhou F, Qin B, Ye R, Shen S, et al. 2011. Crystallographic Realization of the Mathematically Predicted Densest All-Pentagon Packing Lattice by C5-Symmetric "Sticky" Fluoropentamers. *Angewandte Chemie International Edition* 50: 10612-15
50. Ren C, Xu S, Xu J, Chen H, Zeng H. 2011. Planar Macrocyclic Fluoropentamers as Supramolecular Organogelators. *Organic Letters* 13: 3840-43
51. Qin B, Ren C, Ye R, Sun C, Chiad K, et al. 2010. Persistently Folded Circular Aromatic Amide Pentamers Containing Modularly Tunable Cation-Binding Cavities with High Ion Selectivity. *Journal of the American Chemical Society* 132: 9564-66
52. Shen J, Ma W, Yu L, Li J-B, Tao H-C, et al. 2014. Size-dependent patterned recognition and extraction of metal ions by a macrocyclic aromatic pyridone pentamer. *Chemical Communications* 50: 12730-33
53. Ong WQ, Zhao H, Sun C, Wu JE, Wong Z, et al. 2012. Patterned recognition of amines and ammonium ions by a pyridine-based helical oligoamide host. *Chemical Communications* 48: 6343-45
54. Sun C, Ren C, Wei Y, Qin B, Zeng H. 2013. Patterned recognition of amines and ammonium ions by a stimuli-responsive foldamer-based hexameric oligophenol host. *Chemical Communications* 49: 5307-09
55. Qin B, Jiang L, Shen S, Sun C, Yuan W, et al. 2011. Folding-Promoted TBACl-Mediated Chemo- and Regioselective Demethylations of Methoxybenzene-Based Macrocyclic Pentamers. *Organic Letters* 13: 6212-15
56. Du Z, Qin B, Sun C, Liu Y, Zheng X, et al. 2012. Folding-promoted TBAX-mediated selective demethylation of methoxybenzene-based macrocyclic aromatic pentamers. *Organic & Biomolecular Chemistry* 10: 4164-71
57. Zhao H, Shen J, Guo J, Ye R, Zeng H. 2013. A macrocyclic aromatic pyridone pentamer as a highly efficient organocatalyst for the direct arylations of unactivated arenes. *Chemical Communications* 49: 2323-25
58. Lang C, Li W, Dong Z, Zhang X, Yang F, et al. 2016. Biomimetic Transmembrane Channels with High Stability and Transporting Efficiency from Helically Folded Macromolecules. *Angewandte Chemie International Edition* 55: 9723-27
59. Lang C, Deng X, Yang F, Yang B, Wang W, et al. 2017. Highly Selective Artificial Potassium Ion Channels Constructed from Pore-Containing Helical Oligomers. *Angewandte Chemie International Edition* 56: 12668-71
60. Zhao H, Sheng S, Hong Y, Zeng H. 2014. Proton Gradient-Induced Water Transport Mediated by Water Wires Inside Narrow Aquapores of Aquafoldamer Molecules. *Journal of the American Chemical Society* 136: 14270-76
61. Zhao H, Ong WQ, Fang X, Zhou F, Hii MN, et al. 2012. Synthesis, structural investigation and computational modelling of water-binding aquafoldamers. *Organic & Biomolecular Chemistry* 10: 1172-80
62. Schneider S, Licsandru E-D, Kocsis I, Gilles A, Dumitru F, et al. 2017. Columnar Self-Assemblies of Triarylamines as Scaffolds for Artificial Biomimetic Channels for Ion and for Water Transport. *Journal of the American Chemical Society* 139: 3721-27

63. Moulin E, Niess F, Maaloum M, Buhler E, Nyrkova I, Giuseppone N. 2010. The Hierarchical Self-Assembly of Charge Nanocarriers: A Highly Cooperative Process Promoted by Visible Light. *Angewandte Chemie International Edition* 49: 6974-78
64. Nyrkova I, Moulin E, Armao JJ, Maaloum M, Heinrich B, et al. 2014. Supramolecular Self-Assembly and Radical Kinetics in Conducting Self-Replicating Nanowires. *ACS Nano* 8: 10111-24
65. Armao JJ, Maaloum M, Ellis T, Fuks G, Rawiso M, et al. 2014. Healable Supramolecular Polymers as Organic Metals. *Journal of the American Chemical Society* 136: 11382-88
66. Wolf A, Moulin E, Cid J-J, Goujon A, Du G, et al. 2015. pH and light-controlled self-assembly of bistable [c2] daisy chain rotaxanes. *Chemical Communications* 51: 4212-15
67. Armao JJ, Rabu P, Moulin E, Giuseppone N. 2016. Long-Range Energy Transport via Plasmonic Propagation in a Supramolecular Organic Waveguide. *Nano Letters* 16: 2800-05
68. Faramarzi V, Niess F, Moulin E, Maaloum M, Dayen J-F, et al. 2012. Light-triggered self-construction of supramolecular organic nanowires as metallic interconnects. *Nature Chemistry* 4: 485
69. Moulin E, Niess F, Fuks G, Jouault N, Buhler E, Giuseppone N. 2012. Light-triggered self-assembly of triarylamine-based nanospheres. *Nanoscale* 4: 6748-51
70. Busseron E, Cid J-J, Wolf A, Du G, Moulin E, et al. 2015. Light-Controlled Morphologies of Self-Assembled Triarylamine–Fullerene Conjugates. *ACS Nano* 9: 2760-72
71. Gilles A, Barboiu M. 2016. Highly Selective Artificial K+ Channels: An Example of Selectivity-Induced Transmembrane Potential. *Journal of the American Chemical Society* 138: 426-32
72. Sun Z, Barboiu M, Legrand Y-M, Petit E, Rotaru A. 2015. Highly Selective Artificial Cholesteryl Crown Ether K+-Channels. *Angewandte Chemie International Edition* 54: 14473-77
73. Sun Z, Gilles A, Kocsis I, Legrand Y-M, Petit E, Barboiu M. 2016. Squalyl Crown Ether Self-Assembled Conjugates: An Example of Highly Selective Artificial K+ Channels. *Chemistry – A European Journal* 22: 2158-64
74. Barboiu M, Cerneaux S, van der Lee A, Vaughan G. 2004. Ion-Driven ATP Pump by Self-Organized Hybrid Membrane Materials. *Journal of the American Chemical Society* 126: 3545-50
75. Cazacu A, Tong C, van der Lee A, Fyles TM, Barboiu M. 2006. Columnar Self-Assembled Ureido Crown Ethers: An Example of Ion-Channel Organization in Lipid Bilayers. *Journal of the American Chemical Society* 128: 9541-48
76. Barboiu M, Vaughan G, van der Lee A. 2003. Self-Organized Heteroditopic Macrocyclic Superstructures. *Organic Letters* 5: 3073-76
77. Cazacu A, Legrand Y-M, Pasc A, Nasr G, Van der Lee A, et al. 2009. Dynamic hybrid materials for constitutional self-instructed membranes. *Proceedings of the National Academy of Sciences* 106: 8117-22
78. Xue M, Yang Y, Chi X, Zhang Z, Huang F. 2012. Pillararenes, A New Class of Macrocycles for Supramolecular Chemistry. *Accounts of Chemical Research* 45: 1294-308
79. Si W, Li Z-T, Hou J-L. 2014. Voltage-Driven Reversible Insertion into and Leaving from a Lipid Bilayer: Tuning Transmembrane Transport of Artificial Channels. *Angewandte Chemie International Edition* 53: 4578-81
80. Si W, Chen L, Hu X-B, Tang G, Chen Z, et al. 2011. Selective Artificial Transmembrane Channels for Protons by Formation of Water Wires. *Angewandte Chemie International Edition* 50: 12564-68
81. Chen L, Si W, Zhang L, Tang G, Li ZT, Hou JL. 2013. Chiral selective transmembrane transport of amino acids through artificial channels. *J Am Chem Soc* 135: 2152-5
82. Si W, Hu X-B, Liu X-H, Fan R, Chen Z, et al. 2011. Self-assembly and proton conductance of organic nanotubes from pillar[5]arenes. *Tetrahedron Letters* 52: 2484-87
83. Burykin A, Warshel A. 2003. What Really Prevents Proton Transport through Aquaporin?

Charge Self-Energy versus Proton Wire Proposals. *Biophysical Journal* 85: 3696-706
84. Tunuguntla RH, Henley RY, Yao Y-C, Pham TA, Wanunu M, Noy A. 2017. Enhanced water permeability and tunable ion selectivity in subnanometer carbon nanotube porins. *Science* 357: 792
85. Sutera SP, Skalak R. 1993. The History of Poiseuille's Law. *Annual Review of Fluid Mechanics* 25: 1-20
86. Wijmans JG, Baker RW. 1995. The solution-diffusion model: a review. *Journal of Membrane Science* 107: 1-21
87. Beckstein O, Sansom MSP. 2003. Liquid–vapor oscillations of water in hydrophobic nanopores. *Proceedings of the National Academy of Sciences* 100: 7063-68
88. Holt JK, Park HG, Wang Y, Stadermann M, Artyukhin AB, et al. 2006. Fast Mass Transport Through Sub-2-Nanometer Carbon Nanotubes. *Science* 312: 1034-37
89. Hummer G, Rasaiah JC, Noworyta JP. 2001. Water conduction through the hydrophobic channel of a carbon nanotube. *Nature* 414: 188
90. Joseph S, Aluru NR. 2008. Why Are Carbon Nanotubes Fast Transporters of Water? *Nano Letters* 8: 452-58
91. Majumder M, Chopra N, Andrews R, Hinds BJ. 2005. Enhanced flow in carbon nanotubes. *Nature* 438: 44
92. Secchi E, Marbach S, Niguès A, Stein D, Siria A, Bocquet L. 2016. Massive radius-dependent flow slippage in carbon nanotubes. *Nature* 537: 210
93. Fornasiero F, Park HG, Holt JK, Stadermann M, Grigoropoulos CP, et al. 2008. Ion exclusion by sub-2-nm carbon nanotube pores. *Proceedings of the National Academy of Sciences* 105: 17250-55
94. Tabushi I, Kuroda Y, Yokota K. 1982. A,B,D,F-tetrasubstituted β-cyclodextrin as artificial channel compound. *Tetrahedron Letters* 23: 4601-04
95. Verkman AS, Mitra AK. 2000. Structure and function of aquaporin water channels. *American Journal of Physiology - Renal Physiology* 278: F13-F28
96. Grzelakowski M, Cherenet MF, Shen Y-x, Kumar M. 2015. A framework for accurate evaluation of the promise of aquaporin based biomimetic membranes. *Journal of Membrane Science* 479: 223-31
97. Ren T, Erbakan M, Shen Y, Barbieri E, Saboe P, et al. 2017. Membrane Protein Insertion into and Compatibility with Biomimetic Membranes. *Advanced Biosystems* 1: 1700053-n/a
98. Horner A, Zocher F, Preiner J, Ollinger N, Siligan C, et al. 2015. The mobility of single-file water molecules is governed by the number of H-bonds they may form with channel-lining residues. *Science Advances* 1
99. Hu X-B, Chen Z, Tang G, Hou J-L, Li Z-T. 2012. Single-Molecular Artificial Transmembrane Water Channels. *Journal of the American Chemical Society* 134: 8384-87
100. Shen Y-x, Kumar M. 2017. *Artificial Water Channels: Bioinspired and Energy-Efficient Filtration Materials*. Presented at AIChE Annual Meeting, Minneapolis, MN
101. Chung JY, Lee J-H, Beers KL, Stafford CM. 2011. Stiffness, Strength, and Ductility of Nanoscale Thin Films and Membranes: A Combined Wrinkling–Cracking Methodology. *Nano Letters* 11: 3361-65
102. Kim HJ, Choi K, Baek Y, Kim D-G, Shim J, et al. 2014. High-Performance Reverse Osmosis CNT/Polyamide Nanocomposite Membrane by Controlled Interfacial Interactions. *ACS Applied Materials & Interfaces* 6: 2819-29
103. Lee B, Baek Y, Lee M, Jeong DH, Lee HH, et al. 2015. A carbon nanotube wall membrane for water treatment. *Nature Communications* 6: 7109
104. Rangnekar N, Mittal N, Elyassi B, Caro J, Tsapatsis M. 2015. Zeolite membranes - a review and comparison with MOFs. *Chemical Society Reviews* 44: 7128-54
105. Ismail AF, Yean LP. 2003. Review on the development of defect-free and ultrathin-skinned asymmetric membranes for gas separation through manipulation of phase inversion and

rheological factors. *Journal of Applied Polymer Science* 88: 442-51
106. Lee KP, Arnot TC, Mattia D. 2011. A review of reverse osmosis membrane materials for desalination—Development to date and future potential. *Journal of Membrane Science* 370: 1-22
107. Tang CY, Zhao Y, Wang R, Hélix-Nielsen C, Fane AG. 2013. Desalination by biomimetic aquaporin membranes: Review of status and prospects. *Desalination* 308: 34-40
108. Li X, Wang R, Tang C, Vararattanavech A, Zhao Y, et al. 2012. Preparation of supported lipid membranes for aquaporin Z incorporation. *Colloids and Surfaces B: Biointerfaces* 94: 333-40
109. Wang H, Chung T-S, Tong YW, Jeyaseelan K, Armugam A, et al. 2012. Highly Permeable and Selective Pore-Spanning Biomimetic Membrane Embedded with Aquaporin Z. *Small* 8: 1185-90
110. Zhong PS, Chung T-S, Jeyaseelan K, Armugam A. 2012. Aquaporin-embedded biomimetic membranes for nanofiltration. *Journal of Membrane Science* 407-408: 27-33
111. Sun G, Chung T-S, Jeyaseelan K, Armugam A. 2013. Stabilization and immobilization of aquaporin reconstituted lipid vesicles for water purification. *Colloids and Surfaces B: Biointerfaces* 102: 466-71
112. Wang HL, Chung T-S, Tong YW, Jeyaseelan K, Armugam A, et al. 2013. Mechanically robust and highly permeable AquaporinZ biomimetic membranes. *Journal of Membrane Science* 434: 130-36
113. Sun G, Chung T-S, Jeyaseelan K, Armugam A. 2013. A layer-by-layer self-assembly approach to developing an aquaporin-embedded mixed matrix membrane. *RSC Advances* 3: 473-81
114. Sun G, Chung T-S, Chen N, Lu X, Zhao Q. 2013. Highly permeable aquaporin-embedded biomimetic membranes featuring a magnetic-aided approach. *RSC Advances* 3: 9178-84
115. Duong PHH, Chung T-S, Jeyaseelan K, Armugam A, Chen Z, et al. 2012. Planar biomimetic aquaporin-incorporated triblock copolymer membranes on porous alumina supports for nanofiltration. *Journal of Membrane Science* 409-410: 34-43
116. Xie W, He F, Wang B, Chung T-S, Jeyaseelan K, et al. 2013. An aquaporin-based vesicle-embedded polymeric membrane for low energy water filtration. *Journal of Materials Chemistry A* 1
117. Zhao Y, Qiu C, Li X, Vararattanavech A, Shen W, et al. 2012. Synthesis of robust and high-performance aquaporin-based biomimetic membranes by interfacial polymerization-membrane preparation and RO performance characterization. *Journal of Membrane Science* 423-424: 422-28
118. Xia L, Andersen MF, Hélix-Nielsen C, McCutcheon JR. 2017. Novel Commercial Aquaporin Flat-Sheet Membrane for Forward Osmosis. *Industrial & Engineering Chemistry Research* 56: 11919-25
119. Klara SS, Saboe PO, Sines IT, Babaei M, Chiu P-L, et al. 2016. Magnetically Directed Two-Dimensional Crystallization of OmpF Membrane Proteins in Block Copolymers. *Journal of the American Chemical Society* 138: 28-31
120. Kumar M, Grzelakowski M, Zilles J, Clark M, Meier W. 2007. Highly permeable polymeric membranes based on the incorporation of the functional water channel protein Aquaporin Z. *Proceedings of the National Academy of Sciences* 104: 20719-24
121. Kumar M, Habel JEO, Shen Y-x, Meier WP, Walz T. 2012. High-Density Reconstitution of Functional Water Channels into Vesicular and Planar Block Copolymer Membranes. *Journal of the American Chemical Society* 134: 18631-37
122. Darling SB. 2007. Directing the self-assembly of block copolymers. *Progress in Polymer Science* 32: 1152-204
123. Christian DA, Cai S, Bowen DM, Kim Y, Pajerowski JD, Discher DE. 2009. Polymersome carriers: From self-assembly to siRNA and protein therapeutics. *European Journal of Pharmaceutics and Biopharmaceutics* 71: 463-74

124. Discher BM, Won Y-Y, Ege DS, Lee JC-M, Bates FS, et al. 1999. Polymersomes: Tough Vesicles Made from Diblock Copolymers. *Science* 284: 1143-46
125. Krishnamoorthy S, Hinderling C, Heinzelmann H. 2006. Nanoscale patterning with block copolymers. *Materials Today* 9: 40-47
126. Li X, Iocozzia J, Chen Y, Zhao S, Cui X, et al. Functional Nanoparticles Enabled by Block Copolymer Templates: from Precision Synthesis of Block Copolymers to Properties and Applications of Nanoparticles. *Angewandte Chemie International Edition*: n/a-n/a
127. Abetz V. 2015. Isoporous Block Copolymer Membranes. *Macromolecular Rapid Communications* 36: 10-22